A *p*-[^{18}F]Fluoroethoxyphenyl Bicyclic Nucleoside Analogue as a Potential Positron Emission Tomography Imaging Agent for Varicella-Zoster Virus Thymidine Kinase Gene Expression

Satish K. Chitneni,[†] Christophe M. Deroose,[▽,‡] Jan Balzarini,[§] Rik Gijsbers,[⊥] Sofie Celen,[†] Zeger Debyser,[⊥] Luc Mortelmans,[‡] Alfons M. Verbruggen,[†] and Guy M. Bormans*[,†]

Molecular Small Animal Imaging Center (MoSAIC), Laboratory for Radiopharmacy—Faculty of Pharmaceutical Sciences, Department of Nuclear Medicine, Rega Institute for Medical Research, and Division of Molecular Medicine, Katholieke Universiteit Leuven, Leuven, Belgium

Received August 6, 2007

We recently reported a new positron emission tomography (PET) reporter gene, namely, varicella-zoster virus thymidine kinase (VZV-tk) in combination, with carbon-11 or fluorine-18 labeled *m*-alkoxyphenyl bicyclic nucleoside analogues (BCNAs) as PET reporter probes. We now report the synthesis and evaluation of *p*-alkoxyphenyl-BCNA tracers ([^{11}C]-**4** and [^{18}F]-**5**), which are found to be superior to the *m*-alkoxyphenyl-BCNA tracers. In particular, the fluorine-18 labeled tracer ([^{18}F]-**5**, IC_{50} of **5** is 4.2 μM) shows a higher accumulation in VZV-tk expressing cells than the previously reported *m*-methoxyphenyl BCNA. [^{11}C]-**4** and [^{18}F]-**5** were synthesized by heating the phenol precursor **3** with $^{11}CH_3I$ and $^{18}FCH_2CH_2Br$, respectively, as alkylating agents. In vitro evaluation of [^{11}C]-**4** and [^{18}F]-**5** in 293T cells showed about 14- and 54-fold higher uptake, respectively, into VZV-tk gene-transduced cells compared to control cells. LC−MS analysis confirmed the formation of monophosphate derivative of **5** upon catalysis by VZV TK. In vivo studies of this new reporter gene/probe system are in progress.

Introduction

Development of reporter gene systems to monitor gene expression and cell transplantation is the fastest-growing application of positron emission tomography (PET[a]) technology for small-animal research.[1] Herpes simplex virus type 1 thymidine kinase (HSV1-tk) and its mutant HSV1-sr39tk, which shows improved sensitivity to certain antiherpes compounds and HSV-1-tk substrates, are the most extensively studied PET reporter genes (PRGs) in combination with several radiolabeled acycloguanosine and pyrimidine nucleoside analogues as PET reporter probes (PRPs).[2–5] Two receptor PRGs (for the dopamine D2 receptor and the somatostatin receptor, respectively) and one transporter PRG (for the sodium iodide symporter) have been well characterized. However, these PRGs do not meet the requirements for an ideal system because of endogenous expression in certain mammalian tissues that leads to increased background signal or because their endogenous ligands can bind to the receptors, changing the biology of the cells expressing PRGs.[1,6,7]

Chart 1

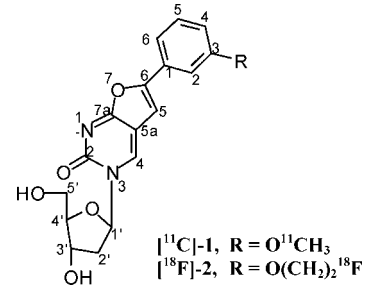

To date, the majority of applications of radionuclide based PRG/PRP technologies have used the HSV1-tk reporter gene, but other herpes virus families, such as varicella-zoster virus (VZV), encode for tk genes (note: tk refers to the gene, and TK refers to the protein) that have different substrate requirements and therefore offer additional windows of opportunity for gene expression imaging.[8] Recently, a new class of antiviral compounds, called bicyclic furopyrimidine deoxynucleoside analogues (BCNAs), was developed by McGuigan et al.[9] BCNAs are highly potent and selective inhibitors of VZV replication.[10] The specificity of BCNAs makes them suitable candidates as PRPs for the VZV-tk reporter gene. Hence, we have synthesized ^{11}C or ^{18}F labeled *m*-alkoxyphenyl-BCNAs **1** and **2** (Chart 1) and studied their biodistribution in normal mice and uptake in VZV-tk expressing human embryonic kidney cells (293T cells).[11] In vitro enzymatic assays using the purified recombinant VZV TK enzyme and nonradioactive **1** or **2** showed that compound **1** has good affinity for the enzyme, with a 50% inhibitory concentration value (IC_{50}) of 4.8 μM. However, compound **2** has poorer affinity for VZV TK (IC_{50} = 53 μM),

* To whom correspondence should be addressed. Address: Onderwijs & Navorsing 2, Herestraat 49, Bus 821, BE-3000 Leuven, Belgium. Phone: +32 16 330447. Fax: +32 16 330449. E-mail: guy.bormans@pharm.kuleuven.be.

▽ Molecular Small Animal Imaging Center.

† Laboratory for Radiopharmacy.

‡ Department of Nuclear Medicine.

§ Rega Institute for Medical Research.

⊥ Division of Molecular Medicine.

[a]Abbreviations: VZV, varicella-zoster virus; tk, thymidine kinase gene; TK, thymidine kinase enzyme; BCNAs, bicyclic nucleoside analogues; HSV1, herpes simplex virus type 1; PET, positron emission tomography; *m*, meta; *p*, para; [^{18}F]-FHBG, 9-(4-[^{18}F]fluoro-3-hydroxymethylbutyl)guanine; BBB, blood−brain barrier; ClogP, calculated log partition coefficient; CC_{50}, 50% cytostatic concentration; 293T cells, human embryonic kidney cells; DMF, dimethylformamide; RP-HPLC, reversed-phase high-performance liquid chromatography; *k*, retention factor; HRMS, high-resolution mass spectrometry; LC−MS, liquid chromatography coupled to mass spectrometry; Da, daltons; *m*/*z*, mass-to-charge ratio; SPE, solid-phase extraction; [^{18}F]FEtBr, [^{18}F]fluoroethyl bromide; [^{11}C]MeI, [^{11}C]methyl iodide; MBq, megabecquerel; kBq, kilobecquerel; IC_{50}, 50% inhibitory concentration; %ID, percent of injected dose; pi, postinjection; SUV, standard uptake value; LV, lentiviral vector; cDNA, complementary DNA; EMCV IRES, encephalomyocarditis virus internal ribosome entry sequence; LV-VZVTK-I-P, lentiviral vector encoding the VZV-tk gene and a puromycin resistance gene (pac, puromycin-*N*-acetyltransferase); NaI(Tl), thallium doped sodium iodide; ES, electrospray ionization; EOS, end of synthesis; EtOH, ethanol; dThd, deoxythymidine; PBS, phosphate-buffered saline.

10.1021/jm700971p CCC: $37.00
Published on Web 11/30/2007

Table 1. Affinity of the Synthesized Nonradioactive Compounds for the Enzymes VZV TK, HSV-1 TK, and Cytosolic TK-1

		IC_{50}[a] (μM)		
compd	R	VZV TK	HSV-1 TK	cytosolic TK-1
3	4-OH	0.4 ± 0.0	>500	>500
4	4-OCH_3	1.5 ± 0.2	>500	>500
5	4-$O(CH_2)_2F$	4.2 ± 0.6	>500	>500
6	4-$O(CH_2)_6F$	4.1 ± 0.1	>500	>500
7	3-$O(CH_2)_6F$	>500	>500	>500

[a] 50% inhibitory concentration or compound concentration required to inhibit nucleoside kinase-catalyzed phosphorylation of 1 μM [CH_3-^{3}H]dThd by 50%.

which was evident in further cell uptake experiments using the radiolabeled tracer [^{18}F]-**2**. The maximum accumulation of [^{11}C]-**1** and [^{18}F]-**2** in 293T cells was respectively 53- and 4.5-fold higher in VZV-tk expressing cells compared to control cells. The accumulation of these tracers in VZV-tk expressing cells suggests that they are specifically phosphorylated by the VZV TK enzyme present in these cells. This system thus constitutes a new combination of a PRG (VZV-tk) and PRP ([^{11}C]-**1**). However, the short half-life ($t_{1/2}$) of carbon-11 (20.4 min) limits the in vivo imaging window to a maximum of about 100 min postinjection (pi), after which insufficient counts are available for statistically meaningful measurements.[12]

2′-Deoxy-2′-[^{18}F]fluoro-5-fluoro-1-β-D-arabinofuranosyluracil ([^{18}F]-FFAU) and 9-(4-[^{18}F]fluoro-3-hydroxymethylbutyl)guanine ([^{18}F]-FHBG) are respectively the most sensitive ([^{18}F]-FFAU) and most extensively studied ([^{18}F]-FHBG) PRPs for imaging HSV1-tk gene expression in animals. They both contain fluorine-18 ($t_{1/2}$ = 110 min) as radionuclide, and PET imaging with [^{18}F]-FHBG has been performed up to more than 2 h pi, by which time the tracer was cleared from the plasma and excreted into the intestines and the urinary bladder, resulting in low background radiation from nontarget organs.[2,3]

For in vivo imaging of the newly developed VZV-tk reporter gene, it can also be assumed that a fluorine-18 labeled PRP must be preferred. However, as described above, [^{18}F]-**2** has lower affinity for VZV TK and accordingly shows less accumulation in VZV-tk expressing cells. The lower affinity of [^{18}F]-**2** compared to [^{11}C]-**1** may indicate that the affinity of VZV TK for these *m*-alkoxyphenyl-BCNAs decreases as the alkyl chain length increases. In order to examine this hypothesis, we have synthesized *m*-fluorohexoxy derivative **7** (Scheme 3), and it indeed shows no measurable affinity even at the highest concentration studied (500 μM, Table 1).

In our search for radiolabeled BCNAs with higher affinity for VZV TK, we have now synthesized stable and radiolabeled *p*-alkoxyphenyl-BCNAs **4** and **5** (Scheme 3). This paper reports their synthesis, their in vitro affinity for VZV TK, their biodistribution, and a study of the in vivo stability of [^{18}F]-**5** in normal mice. Finally, a cell uptake study with radiolabeled **4** and **5** was carried out in VZV-tk expressing 293T cells.

Results and Discussion

Chemistry. The phenolic precursor **3** can be synthesized following the procedure described by McGuigan et al.,[10] which involves a Sonogashira coupling of 4-hydroxyphenylacetylene to 5-iodo-2′-deoxyuridine under cocatalysis of Pd and cuprous ions, followed by copper(I)-promoted in situ cyclization of the coupled product. Alternatively, it can also be synthesized using a coupling reaction between 4-iodophenol and 5-ethynyl-2′-deoxyuridine in the presence of the above-mentioned catalysts. Since the starting material 4-hydroxyphenyl acetylene is less commercially accessible, we have tried the synthesis of **3** following the latter method. However, we obtained mainly a disubstituted analogue with 4-hydroxyphenyl moiety on 5 and 6 positions of the furanopyrimidine base, similar to the earlier report by Luoni et al.[13] Furthermore, it was very difficult to achieve separation of **3** from the 5,6-disubstituted side product. Therefore, we have synthesized *O*-*tert*-butyldimethylsilyl (TBDMS) protected 4-hydroxyphenylacetylene (**10**, Scheme 1) starting from (4-bromophenoxyl)-*tert*-butyldimethylsilane (**8**), following a reported procedure.[14] Initially, compound **8** was treated with trimethylsilyl protected acetylene in dioxane in the presence of catalytic amounts of $PdCl_2(PhCN)_2$, CuI, and tri(*tert*-butyl)phosphane to give compound **9** in 79% yield. Treatment of **9** with $AgNO_3$ as catalyst in acetone containing 100 equiv of water at room temperature (RT) resulted in chemoselective protiodesilylation of the trimethylsilylethynyl group to give compound **10** in 62% yield. Compound **10** was then coupled to 5-iodo-2′-deoxyuridine using Pd and cuprous ions, followed by in situ cyclization in triethylamine and methanol at reflux to obtain the fluorescent *O*-*tert*-butyldimethylsilyl protected compound **12** in moderate yield (46%) (Scheme 2). The deprotection of the phenol group was achieved by treating compound **12** with tetrabutylammonium fluoride (TBAF) in THF to give *p*-hydroxyphenyl-BCNA (**3**) in 73% yield. The reference *O*-methyl derivative **4** was synthesized in 36% yield in the same way as **12** but starting from 4-methoxyphenylacetylene instead of **10.**

The phenol precursor **3** was used as starting material for the synthesis of nonradioactive reference compounds **5** and **6** (Scheme 3). Fluoroalkylation of the phenol precursor (**3**) was achieved by heating with fluoroethyl bromide or fluorohexyl tosylate (**15**) in the presence of potassium carbonate as a base, followed by purification using semipreparative reversed-phase high-performance liquid chromatography (RP-HPLC). Fluorohexyl tosylate (**15**) was synthesized by tosylation of 1,6-hexanediol to yield 1,6-hexanediol bis(*p*-toluenesulfonate) (**14**) in 83% yield,[15] and subsequent fluorination using 1 equiv of TBAF in acetonitrile gave a 70% yield (Scheme 4).

Radiochemistry. The radiosynthesis of **4** and **5** was carried out using compound **3** as precursor and [^{11}C]methyl iodide ([^{11}C]MeI) or [^{18}F]fluoroethyl bromide ([^{18}F]FEtBr) as labeling agents, which were synthesized following reported procedures[16,17] with some modifications. Briefly, [^{11}C]-**4** was synthesized by heating 0.2 mg of the phenol precursor **3** with [^{11}C]MeI in 0.2 mL of DMF in the presence of about 1 mg of Cs_2CO_3 at 90 °C for 8 min. Similarly, [^{18}F]-**5** was prepared by heating the precursor **3** (0.2 mg) with [^{18}F]FEtBr in DMF (0.2 mL) in the presence of about 1 mg of Cs_2CO_3 at 90 °C for 15 min. For both tracers, the synthesis was followed by purification using semipreparative RP-HPLC. The radiochemical purity of both HPLC purified tracers was examined using HPLC on an analytical RP C_{18} column and was always found to be >99%. The identity of the tracers was confirmed by coelution with authentic nonradioactive compounds after coinjection on analytical RP-HPLC, employing 30% acetonitrile in 0.05 M sodium acetate buffer (pH 5.5) as mobile phase at a flow rate of 1 mL/min (Figure 1; [^{11}C]-**4**, retention factor k = 1.19; [^{18}F]-**5**, k = 1.71). The radiochemical yields were 33 ± 1% and 37 ± 2% for [^{11}C]-**4** and [^{18}F]-**5**, respectively (relative to starting radioactivity of [^{11}C]MeI and [^{18}F]FEtBr, respectively, n = 2), and are comparable to the yields of *m*-alkoxyphenyl-BCNA tracers [^{11}C]-**1** and [^{18}F]-**2**.

Partition Coefficient. The lipophilicity of the RP-HPLC purified radiolabeled products was determined by partitioning between 1-octanol and 0.025 M phosphate buffer, pH 7.4 (n =

Scheme 1. Synthesis of *O*-TBDMS Protected 4-Hydroxyphenyl Acetylene (**10**)[a]

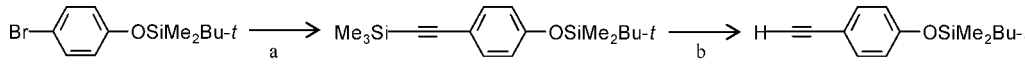

8 **9** **10**

[a] Reaction conditions: (a) Me_3SiCCH, $PdCl_2(PhCN)_2$, $^iPr_2NH$, $^tBu_3P$, CuI, dioxane, RT, 4 h; (b) $AgNO_3$, H_2O, acetone, RT, 44 h.

Scheme 2. Synthesis of Phenol Precursor **3** for Radiolabeling[a]

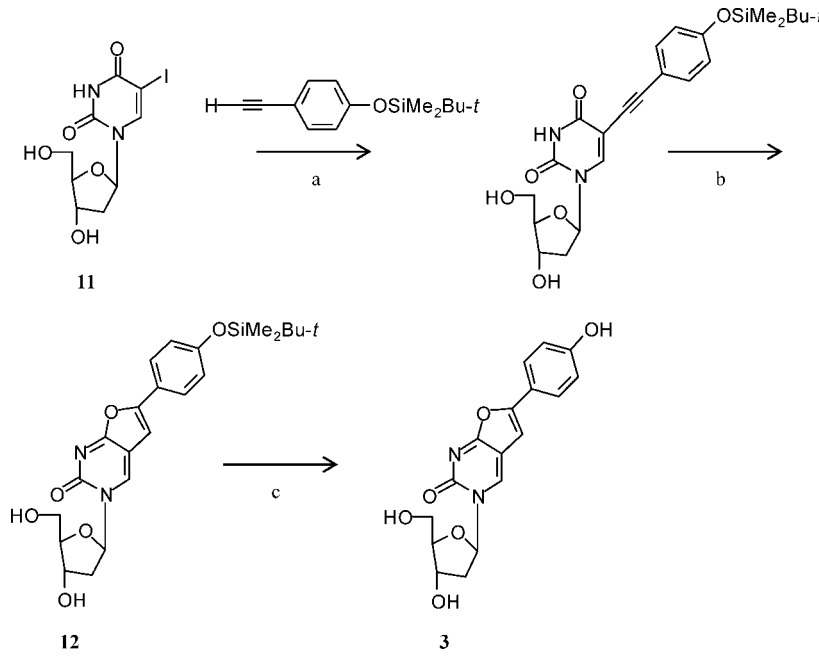

[a] Reaction conditions: (a) $Pd(PPh_3)_4$, $^iPr_2EtN$, CuI, DMF, RT, 19 h; (b) Et_3N/MeOH, CuI, reflux, 4 h; (c) TBAF, THF, RT, 1 h.

Scheme 3. Synthesis of [11C]-**4** and [18F]-**5** and Fluorinated Reference Compounds[a]

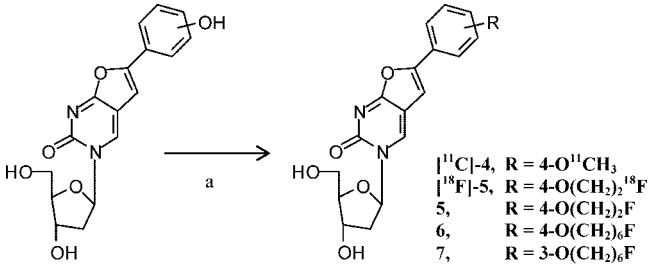

[a] Reaction conditions: (a) $^{11}CH_3I/Br(CH_2)_2{}^{19/18}F/TsO(CH_2)_6F$, base, DMF, Δ.

6). The log of the partition coefficient (log P_{oct}) values of [11C]-**4** and [18F]-**5** were found to be 1.3 and 1.2, respectively.

Affinity of Synthesized Compounds for Kinase Enzymes. The nonradioactive compounds were evaluated for their affinity for purified recombinant VZV TK, HSV-1 TK, and human cytosolic TK-1, and the results are expressed as 50% inhibitory concentration (IC_{50}) values in Table 1. The phenolic precursor **3** displayed the highest affinity for VZV TK, with an IC_{50} value of 0.4 μM. The *O*-methyl and *O*-fluoroethyl derivatives **4** and **5** also exhibited pronounced affinity with IC_{50} values of 1.5 and 4.2 μM, respectively. Unlike *m*-fluorohexoxyphenyl-BCNA (**7**), the *p*-fluorohexoxyphenyl-BCNA **6** also showed good affinity for VZV TK (IC_{50} = 4.1 μM), indicating that the affinity of the para-substituted compounds (**4**−**6**) for VZV TK does not decrease as the alkyl chain length increases and/or that the presence of a fluorine atom does not affect the affinity for the enzyme for the *p*-alkoxyphenyl compounds in contrast to the *m*-alkoxyphenyl derivatives. The affinity of the *p*-fluoroalkoxy derivatives **5** and **6** is comparable to or slightly better than that of the previously reported *m*-methoxyphenyl-BCNA **1** (IC_{50} = 4.8 μM).[11] In contrast to their affinity for VZV TK, the test compounds are not measurably phosphorylated by other nucleoside kinases examined (HSV-1 TK, cytosolic TK-1), with IC_{50} >500 μM (Table 1), which proves the specificity of these compounds for VZV TK.

Biodistribution in Normal Mice. The results of in vivo biodistribution studies of the radiolabeled tracers ([11C]-**4** and [18F]-**5**) in male NMRI mice are presented in Tables 2 and 3 and are similar to those of the *m*-alkoxyphenyl-BCNA tracers [11C]-**1** and [18F]-**2**. Blood clearance was rapid for both tracers (≤1.5% of injected dose (ID) in blood at 60 min postinjection (pi)). The compounds were cleared by the hepatobiliary system (for [11C]-**4** 46.7% and for [18F]-**5** 44.3% of ID in intestines at 60 min pi) and to a lesser extent into the urine (for [11C]-**4** 34.3% and for [18F]-**5** 34.8% of ID in urine at 60 min pi).

Except for liver (4.3–9.9% ID) and intestines (44.3–46.7% ID), the radioactivity in other major organs was negligible at 60 min after injection of the tracers. A significant amount of radioactivity still remained in the carcass even after 60 min pi for [18F]-**5** (11.9% ID). At 2 min pi, the highest concentration of radioactivity was found in the kidneys with standard uptake value (SUV) of 12.3 ± 1.1 for [11C]-**4** and 13.1 ± 7.9 for [18F]-**5**. This was succeeded by liver with SUV values of ≤5.4 for both tracers. At 60 min pi, these values were 1.9 or less for all organs, indicating good clearance of the tracers. As was the case for [11C]-**1** and [18F]-**2**, negligible brain uptake was observed for [11C]-**4** and [18F]-**5** at both 2 and 60 min pi. Hansch and co-workers have suggested that the ideal lipophilicity of neutral molecules for passive diffusion into the central nervous system is log P_{oct} of about 2.[18,19] However, Dischino et al. has

Scheme 4. Synthesis of Fluorohexyl Tosylate **15** [a]

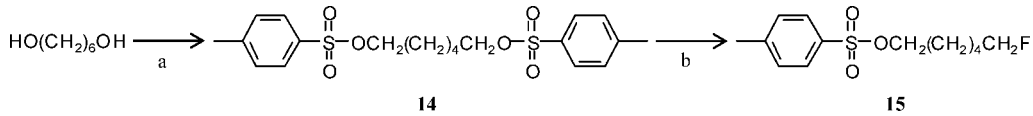

14 **15**

[a] Reaction conditions: (a) tosyl chloride, Et_3N, $Et_3N \cdot HCl$, CH_3CN, 0–5 °C, 1 h; (b) TBAF, CH_3CN, 100 °C, 6 h.

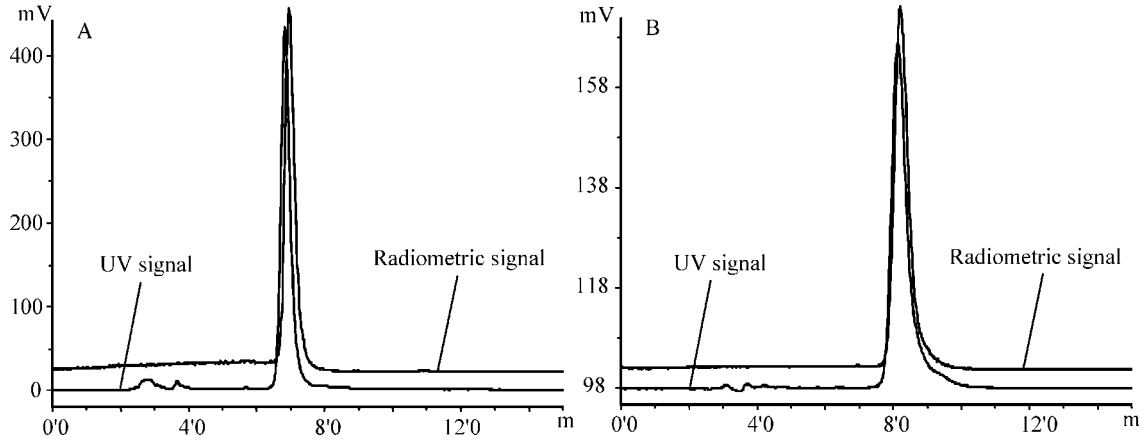

Figure 1. HPLC chromatograms showing the coelution of [^{11}C]-**4** (A) or [^{18}F]-**5** (B) after coinjection with respective authentic nonradioactive compounds.

Table 2. Biodistribution of [^{11}C]-**4** in Normal Mice at 2 and 60 min pi[a]

	%ID[b]		SUV[c]	
organ	2 min	60 min	2 min	60 min
urine	1.4 ± 1.8	34.3 ± 3.1		
kidneys	22.9 ± 1.2	1.4 ± 1.2	12.3 ± 1.1	0.7 ± 0.6
liver	20.3 ± 1.2	9.9 ± 2.4	3.9 ± 0.3	1.9 ± 0.5
spleen + pancreas	1.5 ± 0.2	0.4 ± 0.1	1.5 ± 0.3	0.4 ± 0.0
lungs	1.2 ± 0.2	0.1 ± 0.0	1.3 ± 0.2	0.1 ± 0.0
heart	0.5 ± 0.0	0.0 ± 0.0	0.9 ± 0.1	0.1 ± 0.0
stomach	1.2 ± 0.2	1.0 ± 0.3		
intestines	16.8 ± 1.8	46.7 ± 0.5		
brain	0.0 ± 0.0	0.0 ± 0.0	0.1 ± 0.0	0.0 ± 0.0
blood	7.1 ± 0.7	0.6 ± 0.1	1.0 ± 0.1	0.1 ± 0.0
carcass	29.5 ± 1.3	5.8 ± 0.5		

[a] Data are expressed as the mean ± SD; $n = 3$ per time point. [b] Percentage of injected dose calculated as cpm in organ/total cpm recovered. [c] Standard uptake values calculated as (radioactivity in cpm in organ/weight of the organ (g))/(total counts recovered/body weight (g)).

Table 3. Biodistribution of [^{18}F]-**5** in Normal Mice at 2 and 60 min pi[a]

	%ID[b]		SUV[c]	
organ	2 min	60 min	2 min	60 min
urine	11.8 ± 8.1	34.8 ± 0.3		
kidneys	20.1 ± 10.2	1.1 ± 0.0	13.1 ± 7.9	0.8 ± 0.1
liver	24.7 ± 3.0	4.3 ± 0.8	5.4 ± 0.6	0.8 ± 0.1
spleen + pancreas	1.4 ± 0.1	1.1 ± 0.1	1.7 ± 0.1	1.3 ± 0.2
lungs	0.7 ± 0.3	0.2 ± 0.0	1.3 ± 0.5	0.3 ± 0.1
heart	0.3 ± 0.3	0.1 ± 0.0	1.0 ± 0.9	0.4 ± 0.1
stomach	1.2 ± 0.4	1.1 ± 0.2		
intestines	17.7 ± 3.3	44.3 ± 0.1		
brain	0.0 ± 0.0	0.0 ± 0.0	0.1 ± 0.1	0.0 ± 0.0
blood	4.8 ± 0.8	1.5 ± 0.2	0.7 ± 0.1	0.2 ± 0.0
carcass	18.3 ± 2.9	11.9 ± 0.7		

[a] Data are expressed as mean ± SD; $n = 3$ per time point. [b] Percentage of injected dose calculated as cpm in organ/total cpm recovered. [c] Standard uptake values calculated as (radioactivity in cpm in organ/weight of the organ (g))/(total counts recovered/body weight (g)).

observed that (^{11}C-labeled) compounds with log P_{oct} values between 0.9 and 2.5 were found to pass freely across the blood−brain barrier (BBB).[20] Further, Levin has suggested that the molecular weight limit for a significant entry of a compound into the brain (regardless of lipophilicity) is between 400 and 657 Da.[21] We and several others have been considering these as upper range limits for prediction of BBB penetration of radiotracers.[22,23] In the present study, the log P_{oct} values of [^{11}C]-**4** and [^{18}F]-**5** were 1.3 and 1.2, respectively, both compounds are neutral at physiological pH, and their molecular masses are 358 and 390 Da, respectively. Despite fulfilling the above-mentioned theoretical requirements, [^{11}C]-**4** and [^{18}F]-**5** were not taken up in the brain. We initially hypothesized that the presence of a polar sugar moiety might be detrimental for BBB penetration of these tracers, irrespective of their overall lipophilicity. However, biodistribution studies using ^{11}C-labeled BCNAs, which do not have a sugar moiety or where the 2′-deoxyribose sugar in [^{11}C]-**1** was replaced with a (2-hydroxyethoxy)methyl group (present in the antiherpes drug acyclovir), suggest that the compounds based on the furopyrimidine base system are unable to diffuse over the BBB irrespective of the presence or absence of a sugar moiety because these tracers were also not taken up in the brain.[24] Hence, similar to [^{11}C]-**1**, the newly synthesized tracers ([^{11}C]-**4** and [^{18}F]-**5**) can be useful for imaging VZV infection as well as VZV-tk reporter gene expression in vivo outside the brain only.

Distribution of [^{18}F]-5 between Whole Blood and Plasma. At 2 min after injection of [^{18}F]-**5**, the ratio of radioactivity concentration (%ID/g) in plasma to the radioactivity concentration in whole blood was 1.39 decreased slightly to 1.34 at 10 min pi. At 30 min pi the %ID/g values for plasma and whole blood were almost the same (ratio 1.02). The compound seems to diffuse through the cell membrane of the red blood cells as a function of time pi.

Biostability of [^{18}F]-5. In vivo stability of [^{18}F]-**5** after intravenous (iv) injection in normal mice was assessed by RP-HPLC analysis of plasma at 2, 10, and 30 min pi ($n = 2$ per time point) and of a urine sample at 1 h pi. Samples were analyzed by employing a novel Oasis HLB (hydrophilic–lipophilic balanced) column, without prior precipitation of proteins or removal of other biological matrixes, as described earlier.[11] At 2 min after injection of [^{18}F]-**5**, 94.7 ± 0.3% of the recovered radioactivity in plasma was present as intact tracer and this was at a level of 82.0 ± 2.1% at 10 min pi. However, at 30 min pi

Table 4. In Vitro Incorporation of [11C]-**4** and [18F]-**5** in VZV-tk Gene-Transduced and Control 293T Cells at Time of Maximal uptake (0.5 and 3 h, Respectively)

expt	compd	radioactivity in LV-VZVTK-I-P transduced cells[a]	mean ± SD	radioactivity in control cells[a]	mean ± SD	uptake ratio[b]
1	[11C]-**4**	29.6	28.8 ± 2.6	1.8	2.1 ± 0.5	13.9
2		25.9		2.6		
3		30.8		1.8		
1	[18F]-**5**	67.5	76.6 ± 8.0	1.8	1.4 ± 0.3	53.5
2		79.9		1.3		
3		82.5		1.2		

[a] Data are expressed as % tracer/mg protein. [b] $p < 0.0005$.

only 40.6 ± 4.3% of the recovered radioactivity was in the form of unchanged tracer. A polar metabolite, which eluted in the first wash fraction of the Oasis column (fraction no. 1), was observed during these analyses. The recoveries of HPLC/Oasis column injected radioactivity during these analyses were found to be high with a mean recovery of 91.5 ± 10% ($n = 5$). A urine sample that was collected from a mouse at 1 h pi of [18F]-**5** was also analyzed following the same procedure as that for plasma analysis. Although urine analysis does not require solid-phase extraction (SPE) or workup of the sample prior to the HPLC analysis, use of same online SPE method using an Oasis column for plasma and urine samples enabled us to make a better comparison of the metabolite profile of [18F]-**5** between both samples. On the basis of this analysis, 75.1% of the total radioactivity found in the urine corresponds to [18F]-**5** and 24.9% of the radioactivity was in the form of polar metabolite that was also present in plasma samples. This indicates the metabolism of [18F]-**5** to a polar metabolite in vivo in mice. However, it is important to note here that the metabolism of a radiotracer may differ significantly between different species.[25] Therefore, prior to its use in human studies, metabolite analysis of [18F]-**5** in other animal species such as rats and monkeys is required in order to confirm its in vivo metabolism. In general, BCNAs are not susceptible to breakdown by the nucleoside catabolic enzyme thymidine phosphorylase, which converts many pyrimidine nucleosides into the inactive free base as shown before.[26] On this basis and in view of the very high hydrophilicity of the polar metabolite that was observed in plasma as well as in urine, it is unlikely that this metabolite is the free base of [18F]-**5**.

Uptake of [18F]-5 in Bone and Muscle. The uptake of [18F]-**5** in bone as well as muscle was determined at 2, 10, or 30 min pi of the tracer ($n = 2$ per time point). The %ID/g value for bones was 0.57, 0.66, and 1.25 at 2, 10, and 30 min, respectively. At the same time points the %ID/g values for blood were respectively 1.57, 1.42, and 0.63. Thus, at 30 min pi the bone-to-blood ratio was about 2, indicating the accumulation of 18F activity by bone. Bone uptake of a radiotracer could be attributed to the accumulation of the tracer in the bone marrow and/or free [18F]fluoride in bone matrix after defluorination. Therefore, further studies are required in order to differentiate between bone and marrow uptake of [18F]-**5**. Furthermore, a significant difference was observed between mice and monkeys with regard to defluorination for the widely used HSV1-tk reporter probe [18F]FHBG. For this tracer ([18F]FHBG), a high uptake of [18F] in bone was detected in mice but not in monkeys.[27] On the other hand, the uptake in muscle was minimal and decreased with time (0.35 and 0.25 %ID/g at 2 and 30 min pi, respectively).

In Vitro Evaluation of the Tracers. In vitro evaluation of [11C]-**4** and [18F]-**5** was performed in 293T (human embryonic kidney) cells transduced with human immunodeficiency virus (HIV) type 1 derived lentiviral vector (LV), encoding the VZV-tk gene and a puromycin resistance gene (*pac,* puromycin-N-acetyl-transferase) linked by the encephalomyocarditis virus internal ribosome entry sequence (EMCV IRES), and control cells. The LVs were produced,[28] and cell cultures were transduced as described earlier.[11] Cell lines were denominated LV-VZVTK-I-P or control cells and incubated with [11C]-**4** or [18F]-**5** at 37 °C for different time intervals. It was found that a maximal uptake was observed after 0.5 h of incubation for [11C]-**4** and 3 h of incubation for [18F]-**5**. Further evaluation of cell uptake was done at the respective times of maximal uptake. As shown in Table 4, uptake of [11C]-**4** and [18F]-**5** in the LV-VZVTK-I-P cells was 13.9- and 53.5-fold higher, respectively, than in control cells ($n = 3$; $p < 0.0005$ for both, unpaired bidirectional Student *t* test). Although the affinity of compound **4** for VZV TK is better, the uptake of [11C]-**4** was less than that of [18F]-**5**. The uptake ratio of [18F]-**5** is the same as that of the previously reported [11C]-**1**, and it is 12-fold higher than that of the *m*-fluoroethoxyphenyl-BCNA [18F]-**2**, in the same cell line. Moreover, the accumulation of both [11C]-**4** (28.8%/mg protein) and [18F]-**5** (76.6%/mg protein) is higher than that of [11C]-**1** (12%/mg protein), indicating that the *p*-alkoxyphenyl-BCNA tracers accumulate better than *m*-alkoxyphenyl-BCNA tracers.

HPLC Analysis of Cell Lysate. The specific accumulation of [11C]-**4** and [18F]-**5** in LV-VZVTK-I-P-transduced cells suggests their phosphorylation by the VZV TK enzyme that is present in these cells, in which case the phosphorylated metabolites will be more polar than the parent tracer. In order to evaluate this, the cell lysate that was obtained after incubation of transduced cells with [18F]-**5** for 90 and 180 min (as described in the previous section) was analyzed using RP-HPLC and an Oasis column. As expected, the HPLC profile of the cell lysate (VZV-tk+ cells) at both time points was similar to that of previously reported [11C]-**1**, with recovered radioactivity predominantly present (180 min postincubation) among two hydrophilic components besides the residual parent tracer. The first component was too polar to be retained on the Oasis column and was therefore eluted in the first 3 mL of water rinse (fraction no. 1). The second component eluted between 3 and 4 min (fraction no. 6), while the parent tracer eluted at 8.2 min (in fraction no. 11, as judged from the UV absorption/peak of the coinjected nonradioactive compound **5**). On the basis of reported data on phosphorylation of BCNAs,[29] we assume that the first compound (metabolite b) is the diphosphorylated derivative and the second is the monophosphorylated metabolite (metabolite a), estimated as 17% and 32% of recovered radioactivity, respectively, at 90 min postincubation. At 180 min, the percentage of diphosphorylated metabolite increased to 56%, whereas the monophosphate derivative remained at a similar level (30%; Figure 2). These results are as expected and suggest that [18F]-**5** undergoes monophosphorylation and then diphosphorylation with longer incubation times. This further supports our previous report on [11C]-**1** in which we also described two similar putative mono- and diphosphorylated metabolites.

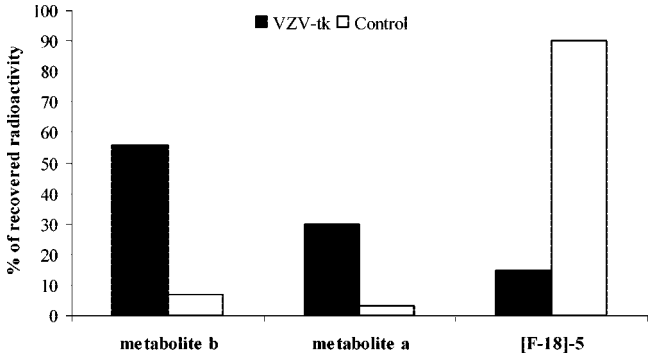

Figure 2. Metabolism of [^{18}F]-**5** in VZV-tk gene-transduced and control 293T cells after 3 h of incubation.

However, [^{18}F]-**5** is converted to the diphosphorylated metabolite (metabolite b) at a higher rate than [^{11}C]-**1** (56% for [^{18}F]-**5** against 27% for [^{11}C]-**1**), presumably because of the longer incubation time for [^{18}F]-**5** (3 h for [^{18}F]-**5** against 30 min for [^{11}C]-**1**). As mentioned above, this indicates a progressive conversion of mono- to diphosphorylated metabolite with longer incubation time. Analysis of the cell lysate from control cells showed no significant presence of metabolite a or b, and ≥90% of the recovered radioactivity corresponded to the parent tracer at 90 and 180 min time points (Figure 2).

Identification of Phosphorylated Metabolite(s) Using Liquid Chromatography Coupled to Mass Spectrometry (LC−MS). Because the control cells only differ from the LV-VZVTK-I-P-transduced cells in their ability to synthesize the VZV TK enzyme, this further supports the hypothesis that the metabolites observed after incubation with the LV-VZVTK-I-P-transduced cells are indeed the mono- and diphosphorylated derivatives of [^{18}F]-**5** and [^{11}C]-**1**. However, in order to achieve accurate identification of these metabolites, we have carried out LC−MS analysis of the incubation reaction mixture (Figure 3). First, the nonradioactive *p*-fluoroethoxyphenyl-BCNA (**5**, 100 μmol) was incubated with purified VZV TK enzyme, similar to the affinity tests but after 5-fold upscale of the ingredients and in the absence of the competitor [CH_3-^{3}H]dThd. After incubation for 2 h at 37 °C the reaction was terminated by adding methanol (final concentration of ∼66%) followed by centrifugation. The incubation mixture was then analyzed using LC−MS, which showed a peak at 13.86 min ($k = 8.8$) with an accurate mass of 389.1152 Da corresponding to the theoretical molecular ion mass of the parent compound **5** (Figure 4A). Similarly, the single ion mass (468.67 ± 0.2 Da, mass corresponding to the monophosphate derivative of **5**) chromatogram showed a relatively polar peak at 10.20 min ($k = 6.2$, Figure 3B) and the accurate mass of this compound was determined to be 469.0801 Da (Figure 4B) corresponding to the theoretical molecular ion mass of the monophosphate derivative, the structure of which is depicted in Figure 5. This experiment confirms the conversion of BCNAs to their phosphate derivatives by the VZV TK enzyme and corroborates that the hydrophilic metabolites observed with [^{18}F]-**5** and [^{11}C]-**1** in VZV-tk expressing cells are indeed the phosphorylated metabolites. The formation of diphosphate derivative of **5** was not observed in these experiments (as evident from RP-HPLC and LC-MS analyses) probably because of the relatively short incubation period. However, this indicates that after phosphorylation, the BCNA monophosphate dissociates from the binding pocket of the VZV TK enzyme before the second phosphorylation step can occur. Although the conversion of BCNAs to their mono- and diphosphates by the VZV TK was demonstrated earlier,[29] it was done by comparing the retention times with those of chemically synthesized reference phosphorylated compounds on RP-HPLC. In the present study we have achieved the direct identity confirmation of the monophosphate formed by the VZV TK mediated catalysis for the first time for this class of compounds.

Conclusion

We have synthesized and evaluated *p*-alkoxyphenyl-BCNA tracers as substrates for the enzyme VZV TK and compared them to previously reported *m*-alkoxyphenyl-BCNAs. In vitro affinity data show that precursor **3** has the highest affinity for VZV TK, followed by the methyl ether **4**. Unlike *m*-fluoroalkoxyphenyl-BCNAs, the ethoxy- and hexoxy-substituted compounds **5** and **6** retained good affinity for VZV TK, indicating that an increase in carbon chain length at the para position is well-tolerated with respect to enzymatic affinity. The loss of enzymatic affinity for the *m*-fluoroalkoxyphenyl-BCNAs might be due to the difference in geometry and steric hindrances of the side chain compared to the *p*-alkoxyphenyl-BCNAs. Although the presence of a long alkyl or alkylaryl side chain is a requirement for the high anti-VZV activity of BCNAs, this could not be modeled into the recently resolved VZV TK structure model without the steric clash with the protein.[30] BCNAs might therefore adopt a different binding mode in VZV TK compared with conventional nucleosides[30] or may induce a change in the three-dimensional structure of the VZV TK protein upon binding. The present work focused on synthesizing fluorine-18 labeled BCNAs that have good affinity for the VZV-tk reporter gene and resulted in the identification of [^{18}F]-**5**, which showed an equal uptake ratio and better accumulation than the previously reported [^{11}C]-**1**. The radiochemical synthesis produced [^{11}C]-**4** and [^{18}F]-**5** in amounts and purity suitable for PET studies. This study also helps to understand the structure–activity relationship (SAR) of alkoxyphenyl-BCNA tracers as substrates for the VZV-tk reporter gene. LC−MS analysis supports the formation of phosphorylated metabolites of BCNAs in the presence of VZV TK. In view of its good affinity for VZV TK, the long half-life of ^{18}F as label compared to ^{11}C, and its higher accumulation rate, [^{18}F]-**5** is the most promising agent for in vivo imaging of VZV-tk. RP-HPLC analysis of plasma and urine samples of mice injected with [^{18}F]-**5** revealed the conversion of this tracer into a more polar metabolite. In vivo studies are in progress in mice bearing VZV-tk expressing xenografts.

Experimental Section

Instruments and General Conditions. For ascending thin layer chromatography (TLC), precoated aluminum backed plates (silica gel 60 with fluorescent indicator, 0.2 mm thickness), supplied by Macherey-Nagel (Düren, Germany), were used and visualization of the spots was performed under UV light (254 or 366 nm). ^{1}H NMR spectra were recorded on a Gemini 300 MHz spectrometer (Varian, Palo Alto, CA) using DMSO-d_6 or $CDCl_3$ as solvent. HPLC purification and analysis were performed on an HPLC system consisting of a Merck Hitachi L6200 intelligent pump (Hitachi, Tokyo, Japan) or a Waters 600 pump (Waters Corporation, Milford, MA) connected to a UV spectrometer (Waters 2487 dual λ absorbance detector) set at 254 nm. For the analysis of radiolabeled compounds, the HPLC eluate after passage through the UV detector was led over a 3 in. NaI(Tl) scintillation detector connected to a single channel analyzer (Medi-Laboratory Select, Mechelen, Belgium). The radioactivity measurements during biodistribution studies, biostability analyses, and cell-uptake studies were done using an automatic γ counter (with a 3 in. NaI(Tl) well crystal) coupled to a multichannel analyzer (Wallac 1480 Wizard 3",

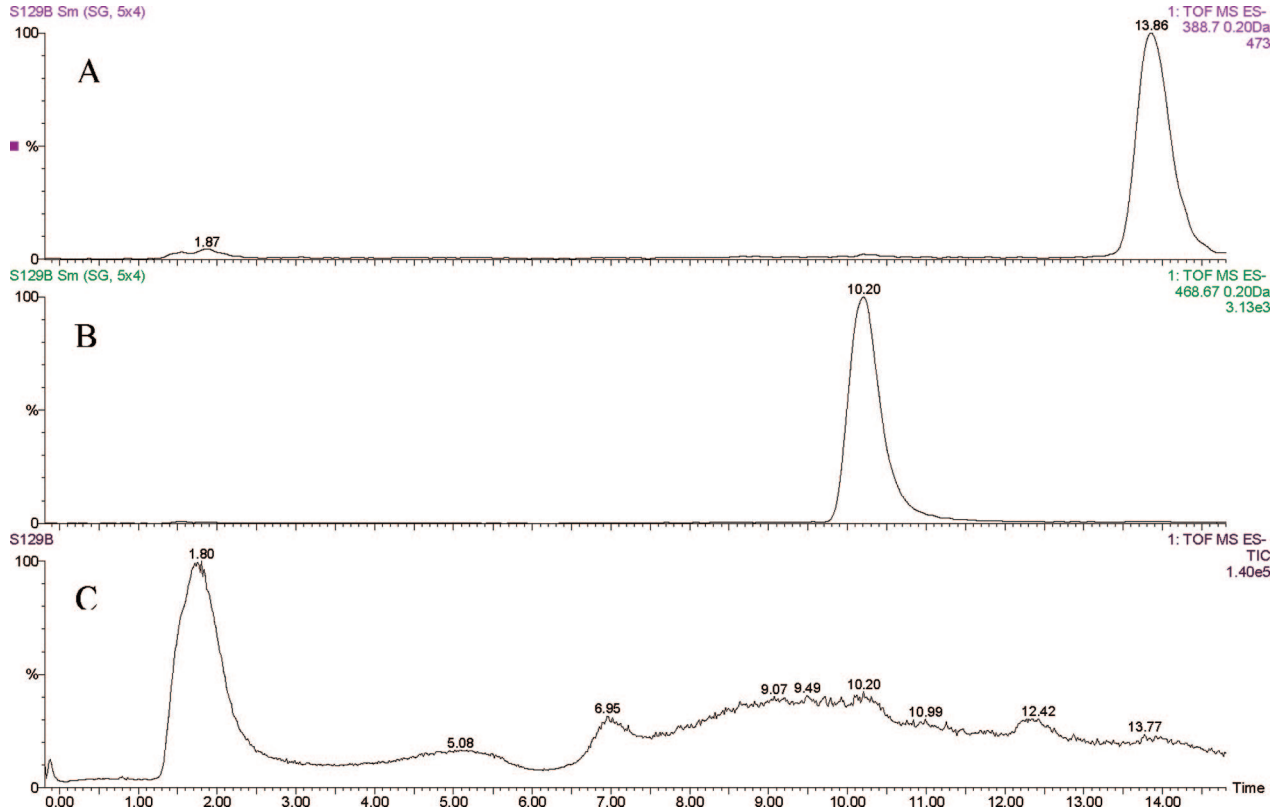

Figure 3. Single ion mass chromatograms for the mass corresponding to unreacted *p*-fluoroethoxyphenyl-BCNA (A; t_R = 13.86 min, k = 8.8) and its monophosphate derivative (B; t_R = 10.20 min, k = 6.2) and the total ion current (TIC) chromatogram (C) of the phosphorylation reaction mixture.

Wallac, Turku, Finland). Mass spectra were recorded on a time-of-flight mass spectrometer (LCT, Micromass, Manchester, U.K.) equipped with an orthogonal electrospray ionization (ESI) interface and operating in positive mode (ES+). Samples were infused in acetonitrile/water using a Harvard 22 syringe pump (Harvard Instruments, MA). Accurate mass determination was done by coinfusion with a 10 μg/mL solution of Kryptofix 222 as an internal calibration standard. Acquisition and processing of data were done using Masslynx software (version 3.5, Waters). LC−MS analysis was performed on a system consisting of a Waters Alliance 2690 separation module connected to an XTerra MS C18 column (3.5 μm, 2.1 mm × 50 mm; Waters) eluted with gradient mixtures of 0.01 M ammonium acetate (pH 7.5)−acetonitrile (100:0 v/v at 0 min, linear gradient to 50:50 v/v in 6 min, isocratic elution with 50:50 v/v till 10 min) at a flow rate of 0.2 mL/min. The HPLC eluate was led through a UV spectrometer (Waters PDA 996) into the time-of-flight mass spectrometer (LCT, Micromass) with an ESI interface operating in negative mode (ES−). For these experiments a 10 μg/mL solution of uridine monophosphate was coinfused with the HPLC eluate into the mass spectrometer as an internal calibration mass. All reagents and solvents were obtained commercially from Acros Organics (Geel, Belgium), Aldrich, Fluka, Sigma (Sigma-Aldrich, Bornem, Belgium), or Fischer Bioblock Scientific (Tournai, Belgium) and used as supplied.

{[4-(*tert*-Butyldimethylsilyloxy)phenyl]ethynyl}trimethylsilane (9). To a stirred solution of bis(benzonitrile)palladium(II) chloride ($PdCl_2(PhCN)_2$) (107 mg, 0.28 mmol) and copper(I) iodide (35 mg, 0.38 mmol) in dioxane (3.5 mL) were sequentially added tri(*tert*-butyl)phosphane (139 μL, 0.56 mmol), (4-bromophenoxyl)-*tert*-butyldimethylsilane (**8**) (2.67 g, 9.3 mmol in 3.5 mL of dioxane), (trimethylsilyl)acetylene (1.54 mL, 11.15 mmol), and diisopropylamine (0.95 mL, 11.12 mmol) under nitrogen at RT. The resulting mixture was stirred at RT for 4 h, and the reaction mixture was diluted with EtOAc (70 mL) and filtered. The filtrate was concentrated under reduced pressure and the residue was purified using column chromatography on silica gel eluted with hexane to give a pale-yellow liquid (2.24 g, 79%).

1-[(*tert*-Butyldimethylsilyl)oxy]-4-ethynylbenzene (10). Water (13 mL, 0.74 mol) and silver nitrate (125 mg, 0.74 mmol) were added to a solution of **9** (2.24 g, 7.35 mmol) in acetone (55 mL), and the resulting mixture was stirred in the dark at RT for 44 h. It was then poured into a saturated aqueous NaCl solution (88 mL) and extracted with diethyl ether (6 × 40 mL). The organic extract was washed with brine (3 × 25 mL), dried, and concentrated under reduced pressure. The residue was purified using column chromatography on silica gel with hexane as eluent to give a colorless liquid (1.1 g, 62%).

3-(2′-Deoxy-β-D-ribofuranosyl)-6-(4-*tert*-butyldimethylsilyloxyphenyl)-2,3-dihydrofuro[2,3-*d*]pyrimidin-2(3*H*)-one (12). To a stirred solution of **10** (1.1 g, 4.58 mmol) in DMF (15 mL) under nitrogen at RT were sequentially added 5-iodo-2′-deoxyuridine (**11**, 1.48 g, 4.17 mmol), *N*,*N*-diisopropylethylamine (1.54 mL, 8.7 mmol), tetrakis(triphenylphosphine)palladium(0) (0.488 g, 0.417 mmol), and copper(I) iodide (0.160 g, 0.83 mmol). The resulting mixture was stirred for 19 h after which TLC showed complete conversion of the starting material. Copper(I) iodide (0.148 g), methanol (37 mL), and triethylamine (27.7 mL) were then added to the reaction mixture, and this was heated under reflux for 4 h. The solvents were evaporated under reduced pressure, and the resulting residue was stirred with Amberlite IRA-400 (HCO_3^-) in CH_3OH/CH_2Cl_2 (1:1) (15 mL) for 1 h. The resin was filtered and washed several times with methanol, and the combined filtrates were evaporated to dryness. The crude product was purified using column chromatography on silica gel eluted with gradient mixtures of CH_2Cl_2 and CH_3OH (up to 8%). Appropriate fractions were combined, and the solvent was removed under reduced pressure to yield a white solid (0.88 g, 46%).

3-(2′-Deoxy-β-D-ribofuranosyl)-6-(4-hydroxyphenyl)-2,3-dihydrofuro[2,3-*d*]pyrimidin-2(3*H*)-one (3). To a stirred solution of **12** (0.77 g, 1.68 mmol) in THF (100 mL) under nitrogen was slowly

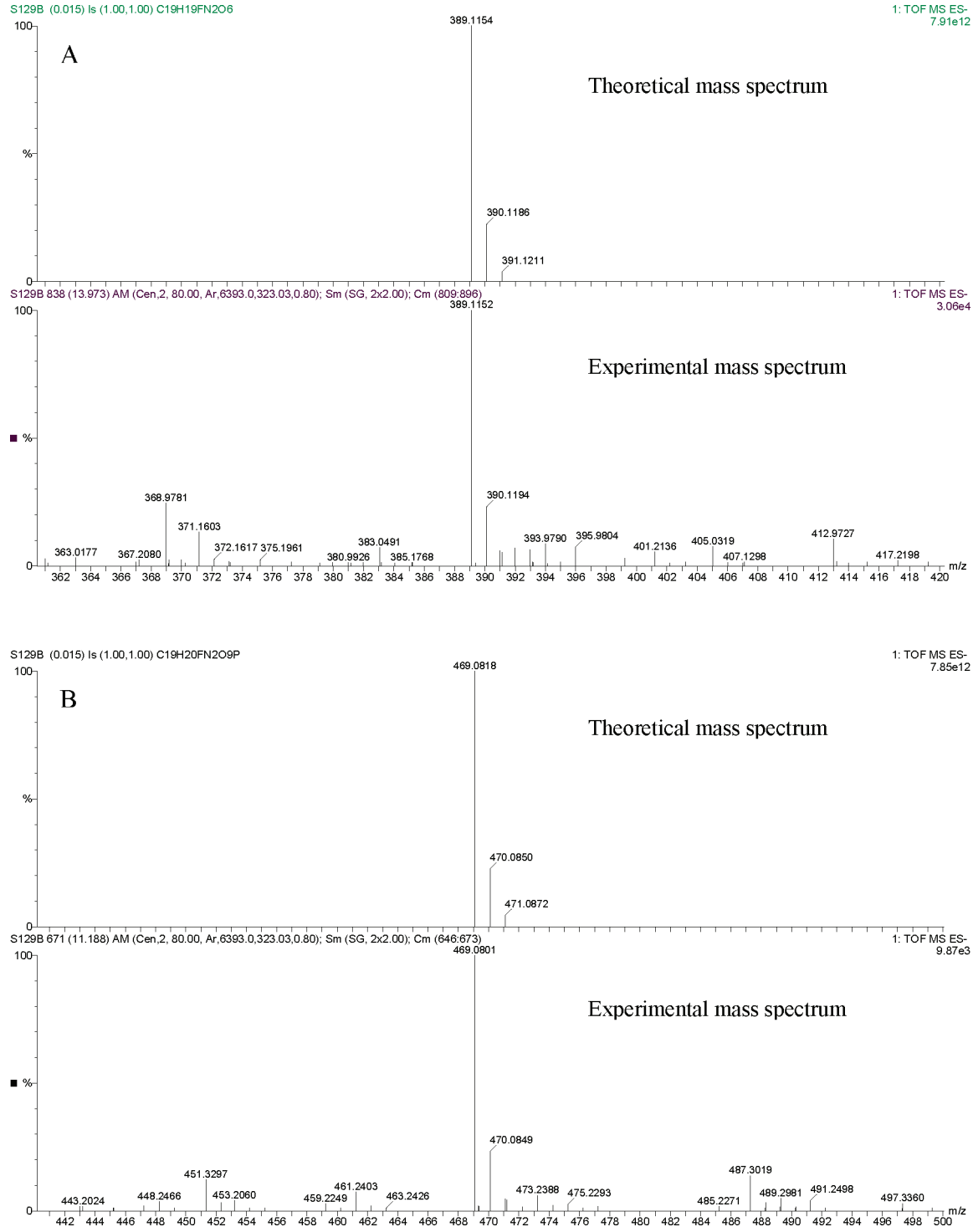

Figure 4. Accurate mass spectra corresponding to the unreacted *p*-fluoroethoxyphenyl-BCNA (A) and its monophosphate derivative (B) after summing the respective peaks in Figure 3 and using uridine monophosphate (*m*/*z* 323.0280) as an internal lock mass.

added tetrabutylammonium fluoride (5.04 mL, 1 M solution in THF). The resulting mixture was stirred at RT for 1 h after which TLC showed complete conversion of the starting material. The crude mixture was filtered. The residue was washed with THF and purified using column chromatography on silica gel eluted with gradient mixtures of CH_2Cl_2 and CH_3OH (up to 12%). Appropriate fractions were combined and the solvent was removed under reduced pressure to yield the product as a yellow solid (0.48 g, 73%).

1,6-Hexanediol Bis(*p*-toluenesulfonate) (14). *p*-Toluenesulfonyl chloride (8 g, 42.25 mmol) in acetonitrile (20 mL) was added dropwise to a solution of 1,6-hexanediol (2.0 g, 16.9 mmol), Et_3N (9.5 mL, 67.6 mmol), and $Et_3N{\cdot}HCl$ (0.32 g, 3.4 mmol) in acetonitrile (17 mL) at 0–5 °C, and the mixture was stirred for 1 h. The reaction was stopped by addition of water, and the solvents were evaporated under reduced pressure. The residue was then dissolved in ethyl acetate (100 mL) and extracted with water (2 × 100 mL). The organic phase was dried ($MgSO_4$) and concentrated. The crude product was purified using column chromatography on silica gel eluted with gradient mixtures of hexane and EtOAc (up to 30%) to yield compound **12** as a white solid (6 g, 83%).

1-Fluoro-6-(*p*-toluenesulfonyl)hexanol (15). Tetrabutylammonium fluoride (4.6 mL, 1 M solution in THF) was added to a solution of **14** (2.0 g, 4.6 mmol) in dry acetonitrile (50 mL), and the reaction mixture was stirred at 100 °C under reflux for 6 h.

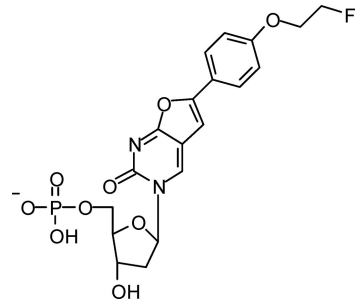

Figure 5. Proposed chemical structure of *p*-fluoroethoxyphenyl-BCNA monophosphate.

The solvent was evaporated under reduced pressure and the residue was purified using column chromatography on silica gel eluted with gradient mixtures of hexane and EtOAc (up to 15%) to yield compound **15** as a pale-yellow oil (0.88 g, 70%).

3-(2′-Deoxy-β-D-ribofuranosyl)-6-(4-methoxyphenyl)-2,3-dihydrofuro[2,3-*d*]pyrimidin-2(3*H*)-one (4). The same procedure was used as described for compound **12** but using 2.82 mmol of **11** and 7.57 mmol of 4-methoxyphenylacetylene. The product was purified using column chromatography on silica gel eluted with gradient mixtures of CH_2Cl_2 and CH_3OH (up to 10%) to yield compound **4** as a white solid (0.37 g, 36%).

3-(2′-Deoxy-β-D-ribofuranosyl)-6-(4-(1-fluoroethoxy)phenyl)-2,3-dihydrofuro[2,3-*d*]pyrimidin-2(3*H*)-one (5). To a solution of **3** (50 mg, 0.145 mmol) in DMF (10 mL) was added K_2CO_3 (41 mg, 0.29 mmol) and 1-bromo-2-fluoroethane (27.6 μL, 0.22 mmol) at RT. The reaction mixture was stirred at 70 °C for 2 h after which a more lipophilic and highly fluorescent spot appeared on TLC. The product was purified by HPLC using a C-18 semipreparative column (Econosphere, 10 mm × 250 mm; Alltech, Deerfield, IL) eluted with water−acetonitrile (75:25, v/v) at a flow rate of 2.5 mL/min ($k = 3.1$). After evaporation of the solvent, the product was obtained as a white solid (30 mg, 53%).

3-(2′-Deoxy-β-D-ribofuranosyl)-6-(4-(1-fluorohexyloxy)phenyl)-2,3-dihydrofuro[2,3-*d*]pyrimidin-2(3*H*)-one (6). The same procedure was used as described for compound **5** but using 1-fluoro-6-(*p*-toluenesulfonyl)hexanol (**15**) instead of 1-bromo-2-fluoroethane. The product was purified by HPLC using a C-18 semipreparative column (Econosphere, 10 mm × 250 mm; Alltech) eluted with 40% acetonitrile in water at a flow rate of 3 mL/min ($k = 3.5$). After evaporation of the solvent, the product was obtained as a white solid (50 mg, 77%).

3-(2′-Deoxy-β-D-ribofuranosyl)-6-(3-(1-fluorohexyloxyphenyl)-2,3-dihydrofuro[2,3-*d*]pyrimidin-2(3*H*)-one (7). The same procedure was used as described for compound **5** but using 3-hydroxyphenyl BCNA as a starting material and 1-fluoro-6-(*p*-toluenesulfonyl)hexanol (**15**) instead of 1-bromo-2-fluoroethane. The product was purified by HPLC using a C-18 semipreparative column (Econosphere, 10 mm × 250 mm; Alltech) eluted with 45% acetonitrile in water at a flow rate of 3 mL/min ($k = 2.0$). After evaporation of the solvent, the product was obtained as a white solid (40 mg, 62%).

Production of [11C]Methyl Iodide and Radiosynthesis of [11C]-4. Carbon-11 was produced by a [14N(p,α)11C] nuclear reaction. The target gas (a mixture of 95% N_2 and 5% H_2) was irradiated using 18 MeV protons from a Cyclone 18/9 cyclotron (Ion Beam Applications, Louvain-la-Neuve, Belgium) at a beam current of 25 μA for about 25 min to yield [11C]CH_4. This was then reacted with vaporous I_2 at 650 °C to convert it to [11C]methyl iodide. The resulting volatile [11C]MeI was bubbled into a reaction vial containing a solution of **3** (0.2 mg) and Cs_2CO_3 (1 mg) in anhydrous DMF (0.2 mL). When maximum radioactivity was trapped, the reaction mixture was heated at 90 °C for 8 min. Volatile impurities and unreacted [11C]MeI were flushed out of the reaction mixture by bubbling it with helium at 50 °C for about 1 min. The crude reaction mixture was diluted with water and applied onto a semipreparative HPLC column (HS HyperPrep RP C_{18}, 100 Å, 8 μm; 10 mm × 250 mm; Alltech) that was eluted with 0.05 M sodium acetate buffer (pH 5.5)/EtOH (65:35, v/v) at a flow rate of 2.5 mL/min ([11C]-**4**, $k = 0.9$). The purity of the labeled tracer was analyzed using RP-HPLC on an XTerra RP C_{18} column (5 μm, 4.6 mm × 250 mm; Waters), eluted with 0.05 M sodium acetate buffer (pH 5.5)−acetonitrile (70:30, v/v) at a flow rate of 1 mL/min ($k = 1.2$). [11C]-**4** was synthesized in 33 ± 1% radiochemical yield (relative to starting [11C]MeI, nondecay-corrected, $n = 2$), and the average specific radioactivity was 98.6 GBq/μmol (2.66 Ci/μmol) at the end of synthesis (EOS).

Production of [18F]Fluoride, [18F]FEtBr, and [18F]-5. [18F]F^- was produced by an [18O(p,n)18F] reaction by irradiation of 0.5 mL of 97% enriched $H_2{}^{18}O$ (Rotem HYOX18, Rotem Industries, Beer Sheva, Israel) in a niobium target using 18 MeV protons and separated from [18O]H_2O using a SepPak Light Accell plus QMA anion exchange cartridge (Waters), which was preconditioned by successive treatments with 0.5 M K_2CO_3 solution (10 mL) and water (2 × 10 mL). The [18F]F^- was then eluted from the cartridge into a reaction vial with a solution containing 2.47 mg of potassium carbonate and 27.9 mg of Kryptofix 222 in 0.75 mL of H_2O-CH_3CN (5:95 v/v).

After evaporation of the solvent, [18F]F^- was further dried by azeotropic distillation of traces of water using acetonitrile. 2-Bromoethyl triflate ($BrCH_2CH_2OTf$) (5 μL) in *o*-dichlorobenzene (0.7 mL) was added into the vial containing [18F]F^-. The reaction vial was then heated to 110 °C, and the resulting [18F]FEtBr was distilled using a flow of helium (3–4 mL/min) into another vial containing a solution of **3** (0.2 mg) and Cs_2CO_3 (1 mg) in anhydrous DMF (0.2 mL). After maximum radioactivity was distilled into the solution, the reaction mixture was heated at 90 °C for 15 min. Volatile impurities and unreacted [18F]FEtBr were evaporated by flushing the mixture with helium at 50 °C until the radioactivity in the vial remained at a stable level. The crude mixture was then diluted with 1.6 mL of water and purified in the same manner as for [11C]-**4**. The product was collected at 10.4 min ($k = 0.7$), while the precursor eluted at 6.4 min ($k = 0.1$). The purity of the labeled tracer was analyzed in the same manner as for [11C]-**4** ($k = 1.7$). The mean decay-corrected radiochemical yield was 37 ± 2% (relative to starting [18F]FEtBr, $n = 2$). Starting from [18F]FEtBr, the synthesis time to obtain the pure product was about 60 min. The average specific activity was found to be 55.4 GBq/μmol (1.50 Ci/μmol) at EOS.

Partition Coefficient Determination. An aliquot of 25 μL of RP-HPLC isolated labeled product containing approximately 550 kBq of [11C]-**4** or 185 kBq of [18F]-**5** was added to a tube containing a mixture of 1-octanol and 0.025 M phosphate buffer, pH 7.4 (2 mL each). The test tube was vortexed at room temperature for 2 min followed by centrifugation at 3000 rpm (1837 g) for 5 min (Eppendorf centrifuge 5810, Eppendorf, Westbury, NY). Aliquots of about 60 and 500 μL were drawn from the 1-octanol and aqueous phases, respectively, taking care to avoid cross-contamination between the two phases, and weighed. The radioactivity in the aliquots was counted using an automatic γ counter. After correction for density and the mass difference between the two phases, the partition coefficient (P) was calculated as the ratio (radioactivity (cpm/mL) in 1-octanol)/(radioactivity (cpm/mL) in phosphate buffer, pH 7.4).

Biodistribution in Normal Mice. Solutions of [11C]-**4** and [18F]-**5** obtained after RP-HPLC purification were diluted using water for injection to have the concentration of EtOH be <5%, and further to a concentration of 37 and 3.7 MBq/mL, respectively. The biodistribution of both tracers was determined in male NMRI mice (weight, 37–43 g). The animal studies were performed according to the Belgian code of practice for the care and use of animals, after approval from the university ethics committee for animals. A volume of 0.1 mL of the diluted tracer solution was injected into the mice via a tail vein, under anesthesia (intraperitoneal injection of 0.1 mL of a solution containing 3 mg of ketamine and 0.225 mg of xylazine). The mice were sacrificed by decapitation at 2 or 60 min after injection ($n = 3$ at each time point). Blood was collected in a tared tube and weighed. All organs and other body

parts were dissected and weighed, and their radioactivity was counted in a γ counter. Results are expressed as %ID (cpm in organ/total cpm recovered) or, where possible, as SUVs. SUVs were calculated as (radioactivity in cpm in organ/weight of the organ)/(total counts recovered/body weight). For calculation of total radioactivity in blood, blood mass was assumed to be 7% of the body mass.

Distribution of [^{18}F]-5 between Whole Blood and Plasma. After intravenous administration of about 11.5 MBq [^{18}F]-**5** into mice, the animals were sacrificed by decapitation at 2, 10, or 30 min pi ($n = 2$ at each time point). Blood was collected into a previously weighed BD vacutainer (containing 7.2 mg of K_2EDTA; BD, Franklin Lakes, NJ), and the radioactivity was measured in a γ counter. The samples were centrifuged at 3000 rpm (1837*g*) for 10 min (Eppendorf centrifuge 5810, Eppendorf) to separate plasma. The plasma was transferred to a 1.5 mL Eppendorf tube followed by weighing and measuring of the radioactivity (γ counter) for remaining blood as well as plasma samples. The disintegrations per minute were converted to MBq normalized by sample weight and the injected dose to obtain %ID/g. The ratio of [^{18}F]-**5** concentration in plasma to concentration in whole blood was calculated by dividing the %ID/g value of plasma by the %ID/g value of blood. After the measurement of radioactivity, the plasma samples were placed on ice until HPLC analysis.

Metabolism of [^{18}F]-5 in Mice. The metabolic stability of [^{18}F]-**5** was studied in normal mice by determination of the relative amounts of the parent tracer and radiolabeled metabolites in plasma samples at different time points and in a urine sample. The plasma samples obtained from the above experiments at 2, 10, or 30 min postinjection of tracer ($n = 2$ per time point) were mixed with 20 μL of a 1 mg/mL solution of authentic **5** and injected onto an Oasis HLB column (4.6 mm × 20 mm, Waters) that was preconditioned by successive washings with acetonitrile and water. The proteins and other biological matrices were rinsed off the Oasis column by pumping water (6 mL), which was collected as two 3-mL fractions (fractions 1 and 2). The outlet of the Oasis column was then connected to an XTerra RP C_{18} column (5 μm, 3.9 mm × 250 mm; Waters), and both columns in series were then eluted using 0.05 M sodium acetate−acetonitrile (70:30 v/v) as the mobile phase at a flow rate of 1 mL/min. After passage through an in-line UV detector, the HPLC eluate was collected in 1 mL fractions and their radioactivity as well as the activity in fractions 1 and 2 was measured using a γ counter. Recoveries were calculated on the basis of the amount of radioactivity (number of CPMs) injected onto the Oasis column/HPLC and the amount of radioactivity (number of CPMs) recovered from wash fractions as well as 1 mL eluate fractions after HPLC analysis. A urine sample was collected at 60 min pi by manual voiding of the bladder, mixed with authentic **5**, and analyzed following the same procedure, without any pretreatment or workup.

Uptake of [^{18}F]-5 in Bone and Muscle. The bone and muscle uptake of [^{18}F]-**5** was studied in normal mice at 2, 10, or 30 min pi after injection of 11.5 MBq of the tracer (two animals at each time point). After sacrifice at the specified time point, the femur and the muscle were collected separately and weighed and their radioactivity was measured in a γ counter. The uptake was calculated by determining the %ID/g for the left as well as for the right bone and muscle for all the mice at the above-mentioned time points.

Affinity of Test Compounds for Nucleoside Kinase Enzymes in Vitro. The 50% inhibitory concentration (IC_{50}) of the test compounds against phosphorylation of [CH_3-^{3}H]dThd as the natural substrate for VZV TK, HSV-1 TK, and cytosolic TK-1 was determined. Briefly, the activity of purified recombinant nucleoside kinase enzymes was assayed in a 50 μL reaction mixture containing 50 mM Tris-HCl, pH 8.0, 2.5 mM $MgCl_2$, 10 mM dithiothreitol, 2.5 mM ATP, 1.0 mg/mL bovine serum albumin, 10 mM NaF, [CH_3-^{3}H]dThd (3.7 kBq in 5 μL, 1 μM final concentration), and 5 μL of recombinant enzyme (containing 7.75 ng of VZV TK or 226 ng of HSV-1 TK or 455 ng of TK-1 protein). The samples were incubated at 37 °C for 30 min in the presence or absence of different concentrations of the test compounds. During this time period, the enzymatic reaction proceeded linearly. Aliquots of 45 μL of the reaction mixtures were spotted on Whatman DE-81 filter paper disks (Whatman, Maidstone, U.K.). The filters were washed three times for 5 min in 1 mM ammonium formate and once for 5 min in ethanol. The radioactivity on the filters was determined by liquid scintillation counting.

Cell-Uptake Studies. A lentiviral vector (LV) encoding the cDNA of VZV-tk linked to the puromycin-*N*-acetyltransferase (*pac*) gene through an encephalomyocarditis virus internal ribosome entry sequence (IRES) was produced and denominated LV-VZVTK-I-P. Human embryonic kidney cells (293T) transduced with LV-VZVTK-I-P were maintained in cell culture medium containing 1 μg/mL puromycin. LV-VZVTK-I-P and control cells (293T) were plated in triplicate at a density of 200 000 cells per well in 24-well plates. After 24 h, the medium was discarded and 0.25 mL of fresh medium with HPLC-purified tracer (1.1 MBq [^{11}C]-**4** or 185 kBq [^{18}F]-**5** per well) was added. The cells were then incubated at 37 °C for 3 h for [^{18}F]-**5** and 0.5 h for [^{11}C]-**4**. Following incubation and removal of medium, the cells were washed three times with 0.4 mL of ice-cold phosphate-buffered saline (PBS). The cells were then lysed with 0.25 mL of cell culture lysis reagent 1× solution (Promega Corporation, Madison, WI) for 10 min after which the lysate was collected, followed by a 0.125 mL rinse using the same solution. The cell fractions (lysate and rinse) as well as the wash fractions (medium and PBS) were collected separately for each well, and the radioactivity was measured using a γ counter. The protein concentration of each cell fraction was determined using the Bio-Rad protein assay (Biorad, München, Germany) and a spectrophotometer (Bio Synchron-Anthos 2010, Anthos LabTec Instruments, Austria) at 595 nm. The tracer uptake was normalized for total protein content in the cell fraction for each individual well and expressed as a percentage of total radioactivity per milligram of protein.

HPLC Analysis of [^{18}F]-5 Metabolites from VZV-tk-Gene-Transduced and Control 293T Cells. The cell lysate from the three individual wells from above cell uptake experiments was pooled together for both VZV-tk expressing and control cells at 90 or 180 min after incubation with [^{18}F]-**5**. An amount of 0.9 mL of this pooled cell lysate was mixed with 20 μL of a 1 mg/mL solution of reference compound **5** and injected onto a preconditioned (as described above) Oasis cartridge. The proteins and other biological matrices were rinsed off the Oasis column by elution with 6 mL of water (1 mL/min flow rate), and the eluate was collected as two 3-mL fractions (fractions 1 and 2). The outlet of the Oasis column was then connected to an XTerra RP C_{18} column (5 μm, 4.6 mm × 250 mm; Waters). The two columns in series were eluted using 0.05 M sodium acetate−acetonitrile (70:30 v/v) as the mobile phase at a flow rate of 1 mL/min. The HPLC eluate was collected as 1 mL fractions, and the radioactivity of all fractions was measured using a γ counter (**5**, $k = 1.7$, fraction no. 11).

Acknowledgment. The technical assistance of Lizette van Berckelaer and Ria Van Berwaer is gratefully acknowledged. We thank Marva Bex, Peter Vermaelen, Humphrey Fonge, and Christelle Terwinghe for their help during the experiments. This work was supported by an SBO grant (Grant IWT-30 238) of the Flemish Institute supporting Scientific-Technological Research in industry (IWT), an IDO grant (Grant IDO/02/012) of the Katholieke Universiteit Leuven, and in part the EC (FP6 Project DiMI LSHB-CT-2005-512146).

Supporting Information Available: Data on ^{1}H NMR, HRMS, and HPLC analysis for the synthesized intermediates and final products. This material is available free of charge via the Internet at http://pubs.acs.org.

References

(1) Herschman, H. R. Micro-PET imaging and small animal models of disease. *Curr. Opin. Immunol.* **2003**, *15*, 378–384.

(2) Gambhir, S. S.; Bauer, E.; Black, M. E.; Liang, Q.; Kokoris, M. S.; Barrio, J. R.; Iyer, M.; Namavari, M.; Phelps, M. E.; Herschman, H. R. A mutant herpes simplex virus type 1 thymidine kinase reporter gene shows improved sensitivity for imaging reporter gene expression with positron emission tomography. *Proc. Natl. Acad. Sci. U.S.A.* **2000**, *97*, 2785–2790.
(3) Tjuvajev, J. G.; Doubrovin, M.; Akhurst, T.; Cai, S. D.; Balatoni, J.; Alauddin, M. M.; Finn, R.; Bornmann, W.; Thaler, H.; Conti, P. S.; Blasberg, R. G. Comparison of radiolabeled nucleoside probes (FIAU, FHBG, and FHPG) for PET imaging of HSV1-tk gene expression. *J. Nucl. Med.* **2002**, *43*, 1072–1083.
(4) Alauddin, M. M.; Shahinian, A.; Park, R.; Tohme, M.; Fissekis, J. D.; Conti, P. S. Synthesis and evaluation of 2′-deoxy-2′-F-18-fluoro-5-fluoro-1-beta-D-arabinofuranosyluracil as a potential PET imaging agent for suicide gene expression. *J. Nucl. Med.* **2004**, *45*, 2063–2069.
(5) Yaghoubi, S. S.; Couto, M. A.; Chen, C. C.; Polavaram, L.; Cui, G. G.; Sen, L. Y.; Gambhir, S. S. Preclinical safety evaluation of F-18-FHBG: a PET reporter probe for imaging herpes simplex virus type 1 thymidine kinase (HSV1-tk) or mutant HSV1-sr39tk's expression. *J. Nucl. Med.* **2006**, *47*, 706–715.
(6) Herschman, H. R. PET reporter genes for noninvasive imaging of gene therapy, cell tracking and transgenic analysis. *Crit. Rev. Oncol. Hematol.* **2004**, *51*, 191–204.
(7) Serganova, I.; Blasberg, R. Reporter gene imaging: potential impact on therapy. *Nucl. Med. Biol.* **2005**, *32*, 763–780.
(8) Wiebe, L. I.; Knaus, E. E. Enzyme-targeted, nucleoside-based radiopharmaceuticals for scintigraphic monitoring of gene transfer and expression. *Curr. Pharm. Des.* **2001**, *7*, 1893–1906.
(9) McGuigan, C.; Yarnold, C. J.; Jones, G.; Velazquez, S.; Barucki, H.; Brancale, A.; Andrei, G.; Snoeck, R.; De Clercq, E.; Balzarini, J. Potent and selective inhibition of varicella-zoster virus (VZV) by nucleoside analogues with an unusual bicyclic base. *J. Med. Chem.* **1999**, *42*, 4479–4484.
(10) McGuigan, C.; Barucki, H.; Blewett, S.; Carangio, A.; Erichsen, J. T.; Andrei, G.; Snoeck, R.; De Clercq, E.; Balzarini, J. Highly potent and selective inhibition of varicella-zoster virus by bicyclic furopyrimidine nucleosides bearing an aryl side chain. *J. Med. Chem.* **2000**, *43*, 4993–4997.
(11) Chitneni, S. K.; Deroose, C. M.; Balzarini, J.; Gijsbers, R.; Celen, S. J. L.; de Groot, T. J.; Debyser, Z.; Mortelmans, L.; Verbruggen, A. M.; Bormans, G. M. Synthesis and preliminary evaluation of ^{18}F or ^{11}C labeled bicyclic nucleoside analogues as potential probes for imaging varicella-zoster virus thymidine kinase gene expression using positron emission tomography. *J. Med. Chem.* **2007**, *50*, 1041–1049.
(12) Wilson, A. A.; Dasilva, J. N.; Houle, S. Synthesis of two radiofluorinated cocaine analogues using distilled 2-[^{18}F]fluoroethyl bromide. *Appl. Radiat. Isot.* **1995**, *46*, 765–770.
(13) Luoni, G.; McGuigan, C.; Andrei, G.; Snoeck, R.; De Clercq, E.; Balzarini, J. Bicyclic nucleoside inhibitors of varicella-zoster virus: the effect of branching in the *p*-alkylphenyl side chain. *Bioorg. Med. Chem. Lett.* **2005**, *15*, 3791–3796.
(14) Carpita, A.; Mannocci, L.; Rossi, R. Silver(I)-catalysed protiodesilylation of 1-(trimethylsilyl)-1-alkynes. *Eur. J. Org. Chem.* **2005**, 1859–1864.
(15) Yoshida, Y.; Sakakura, Y.; Aso, N.; Okada, S.; Tanabe, Y. Practical and efficient methods for sulfonylation of alcohols using Ts(Ms)Cl/Et_3N and catalytic $Me_3N\cdot HCl$ as combined base: promising alternative to traditional pyridine. *Tetrahedron* **1999**, *55*, 2183–2192.
(16) Zhang, M. R.; Tsuchiyama, A.; Haradahira, T.; Yoshida, Y.; Furutsuka, K.; Suzuki, K. Development of an automated system for synthesizing ^{18}F-labeled compounds using [^{18}F]fluoroethyl bromide as a synthetic precursor. *Appl. Radiat. Isot.* **2002**, *57*, 335–342.
(17) Larsen, P.; Ulin, J.; Dahlstrom, K.; Jensen, M. Synthesis of [^{11}C]iodomethane by iodination of [^{11}C]methane. *Appl. Radiat. Isot.* **1997**, *48*, 153–157.
(18) Hansch, C.; Steward, A. R.; Anderson, S. M.; Bentley, D. The parabolic dependence of drug action upon lipophilic character as revealed by a study of hypnotics. *J. Med. Chem.* **1968**, *11*, 1–11.
(19) Glave, W. R.; Hansch, C. Relationship between lipophilic character and anesthetic activity. *J. Pharm. Sci.* **1972**, *61*, 589–591.
(20) Dischino, D. D.; Welch, M. J.; Kilbourn, M. R.; Raichle, M. E. Relationship between lipophilicity and brain extraction of C-11-labeled radiopharmaceuticals. *J. Nucl. Med.* **1983**, *24*, 1030–1038.
(21) Levin, V. A. Relationship of octanol/water partition coefficient and molecular weight to rat brain capillary permeability. *J. Med. Chem.* **1980**, *23*, 682–684.
(22) Vanbilloen, H. P.; Kieffer, D. M.; Cleynhens, B. J.; Bormans, G. M.; Mortelmans, L.; Verbruggen, A. M. Evaluation of ^{99m}Tc-labeled tropanes with alkyl substituents on the 3β-phenyl ring as potential dopamine transporter tracers. *Nucl. Med. Biol.* **2006**, *33*, 413–418.
(23) Elsinga, P. H.; Hendrikse, N. H.; Bart, J.; van Waarde, A.; Vaalburg, W. Positron emission tomography studies on binding of central nervous system drugs and P-glycoprotein function in the rodent brain. *Mol. Imaging Biol.* **2005**, *7*, 37–44.
(24) Chitneni, S. K.; Balzarini, J.; Celen, S.; Dyubankova, N.; Verbruggen, A. M.; Bormans, G. M. Relation between structure and brain uptake of carbon-11 labeled acyclic and furo[2,3-*d*]pyrimidine-derivatives of bicyclic nucleoside analogues (BCNAs). Unpublished data.
(25) Kida, T.; Noguchi, J.; Zhang, M. R.; Suhara, T.; Suzuki, K. Metabolite analysis of [^{11}C]Ro15-4513 in mice, rats, monkeys and humans. *Nucl. Med. Biol.* **2003**, *30*, 779–784.
(26) Balzarini, J.; Sienaert, R.; Liekens, S.; Van Kuilenburg, A.; Carangio, A.; Esnouf, R.; De Clercq, E.; McGuigan, C. Lack of susceptibility of bicyclic nucleoside analogs, highly potent inhibitors of varicella-zoster virus, to the catabolic action of thymidine phosphorylase and dihydropyrimidine dehydrogenase. *Mol. Pharmacol.* **2002**, *61*, 1140–1145.
(27) Alauddin, M. M.; Shahinian, A.; Gordon, E. M.; Bading, J. R.; Conti, P. S. Preclinical evaluation of the penciclovir analog 9-(4-[F-18] fluoro-3-hydroxymethylbutyl)guanine for in vivo measurement of suicide gene expression with PET. *J. Nucl. Med.* **2001**, *42*, 1682–1690.
(28) Geraerts, M.; Michiels, M.; Baekelandt, V.; Debyser, Z.; Gijsbers, R. Upscaling of lentiviral vector production by tangential flow filtration. *J. Gene Med.* **2005**, *7*, 1299–1310.
(29) Sienaert, R.; Naesens, L.; Brancale, A.; De Clercq, E.; McGuigan, C.; Balzarini, J. Specific recognition of the bicyclic pyrimidine nucleoside analogs, a new class of highly potent and selective inhibitors of varicella-zoster virus (VZV), by the VZV-encoded thymidine kinase. *Mol. Pharmacol.* **2002**, *61*, 249–254.
(30) Bird, L. E.; Ren, J.; Wright, A.; Leslie, K. D.; Degreve, B.; Balzarini, J.; Stammers, D. K. Crystal structure of varicella-zoster virus thymidine kinase. *J. Biol. Chem.* **2003**, *278*, 24680–24687.

JM700971P